MCB
Journals.ASM.org

p21-Activated Kinase 2 Regulates Endothelial Development and Function through the Bmk1/Erk5 Pathway

Maria Radu,[a] Karen Lyle,[b]* Klaus P. Hoeflich,[c]* Olga Villamar-Cruz,[a]* Hartmut Koeppen,[b] Jonathan Chernoff[a]

Cancer Biology Program, Fox Chase Cancer Center, Philadelphia, Pennsylvania, USA[a]; Department of Research Pathology, Genentech, South San Francisco, California, USA[b]; Department of Translational Oncology, Genentech, South San Francisco, California, USA[c]

p21-activated kinases (Paks) have been shown to regulate cytoskeleton rearrangements, cell proliferation, attachment, and migration in a variety of cellular contexts, including endothelial cells. However, the role of endothelial Pak in embryo development has not been reported, and currently, there is no consensus on the endothelial function of individual Pak isoforms, in particular p21-activated kinase 2 (Pak2), the main Pak isoform expressed in endothelial cells. In this work, we employ genetic and molecular studies that show that Pak2, but not Pak1, is a critical mediator of development and maintenance of endothelial cell function. Endothelial depletion of Pak2 leads to early embryo lethality due to flawed blood vessel formation in the embryo body and yolk sac. In adult endothelial cells, Pak2 depletion leads to severe apoptosis and acute angiogenesis defects, and in adult mice, endothelial Pak2 deletion leads to increased vascular permeability. Furthermore, ubiquitous Pak2 deletion is lethal in adult mice. We show that many of these defects are mediated through a newly unveiled Pak2/Bmk1 pathway. Our results demonstrate that endothelial Pak2 is essential during embryogenesis and also for adult blood vessel maintenance, and they also pinpoint the Bmk1/Erk5 pathway as a critical mediator of endothelial Pak2 signaling.

The p21-activated kinases (Paks) are evolutionarily conserved serine/threonine kinases that act downstream of the Rho family GTPases, Rac1 and Cdc42, to regulate numerous cellular processes. p21-activated kinase 1 (Pak1) to Pak3, the group I Paks, are expressed in numerous tissues with Pak1 being predominantly expressed in brain, muscle, gastrointestinal tract, and thyroid and Pak3 being predominantly expressed in brain (1, 2). Compared to the more restricted expression of Pak1 and Pak3, Pak2 is ubiquitously expressed (3–9). Group I Pak family members share a high degree of homology (3), but they may play distinct roles as observed by the significantly different phenotypes of knockout (KO) animal models. While *Pak1* KO and *Pak3* KO mice are viable (10, 11), *Pak2* KO mice are embryonic lethal at embryonic day 8.5 (E8.5) due to multiple developmental abnormalities, including cardiovascular defects (12).

The role of Pak in endothelial cell (EC) signaling has been studied in animal models (5, 13) and cultured cells (6, 10, 14, 15). Pak signaling is critical in regulating EC attachment, migration, and lumen formation (4-9). Furthermore, Paks have been implicated in maintaining the integrity of the endothelial barrier, but conflicting data implicate various Pak isoforms as both positive and negative regulators of maintaining barrier function (5, 13, 14, 16).

A few *in vivo* studies have specifically implicated Pak2 in vascular pathways. A study in *Danio rerio* showed that *pak2a*, one of two Pak2 orthologs in this organism, plays an important role in cerebral vascular maintenance (5). In this study, chemical mutagenesis of the *pak2a* gene and *pak2a*-targeting morpholinos caused cerebral hemorrhage, implicating this Pak family member in vascular barrier maintenance. In mice, germ line deletion of *Pak2* is embryonic lethal, and embryos display a phenotype that is consistent with vascular defects (12). While these studies suggest that Pak2 may have an essential role in the vasculature, they do not address the endothelial autonomous function of Pak2, since they relied on global *Pak2* deletion in the organism.

To study the role of Pak2 in EC signaling *in vivo*, we generated temporal and tissue-specific conditional *Pak2* KO mice. In this article, we present data that suggests that endothelial Pak2 expression is a critical requirement for embryo viability and morphogenesis of embryonic and extraembryonic vasculature. In adult mice, inducible endothelial *Pak2* KO causes an increase in vascular leaks in the lung and skin. *In vitro* studies using primary mouse and human ECs show that *Pak2* is required for normal cell proliferation, attachment, migration, and sprouting. *Pak2* deletion in ECs is underlined by severe cytoskeletal rearrangements as well as by abnormal signaling through Bmk1/Erk5, also known as mitogen-activated protein kinase 7 (MAPK7), and these defects can be partly suppressed by expression of activated Mek5. Our data show that *Pak2* is essential during developmental angiogenesis and also for mature vessel homeostasis and reveal an unexpected link between Pak2 signaling and the Bmk1/Erk5 pathway.

MATERIALS AND METHODS

Mice. B/6SJL.Tg, C57BL/6J, and Tie2-Cre mice were obtained from The Jackson Laboratory, Bar Harbor, ME. *CreER*^{T2} mice were a generous gift

Received 23 June 2015 **Returned for modification** 14 July 2015
Accepted 8 September 2015

Accepted manuscript posted online 21 September 2015

Citation Radu M, Lyle K, Hoeflich KP, Villamar-Cruz O, Koeppen H, Chernoff J. 2015. p21-activated kinase 2 regulates endothelial development and function through the Bmk1/Erk5 pathway. Mol Cell Biol 35:3990–4005. doi:10.1128/MCB.00630-15.

Address correspondence to Jonathan Chernoff, Jonathan.Chernoff@fccc.edu.

* Present address: Karen Lyle, Stemcentrx, Regulatory Affairs, South San Francisco, California, USA; Klaus P. Hoeflich, Blueprint Medicines, Cambridge, Massachusetts, USA; Olga Villamar-Cruz, Unidad de Biomedicina, Facultad de Estudios Superiores Iztacala, Universidad Nacional Autónoma de México, Tlalnepantla, MEX, Mexico.

M.R. and K.L. contributed equally to this work.

Supplemental material for this article may be found at http://dx.doi.org/10.1128/MCB.00630-15.

from Erica Golemis, Fox Chase Cancer Center, and *VEC-CreER^{T2}* mice were obtained from Luisa Iruela-Arispe, University of California at Los Angeles (UCLA) (17). *Pak1* knockout (KO) mice have been previously described (10). *Pak2$^{fl/wt}$* mice were bred for more than 10 generations to C57BL/6J mice to obtain pure *Pak2$^{fl/+}$* mice with C57BL/6J background. *CreER^{T2}*; *Pak2$^{fl/wt}$* mice were backcrossed for more than 5 generations to the *Pak2$^{fl/+}$* mice with C57BL/6J background. The *VEC-CreER^{T2}* mice were crossed with *Pak2$^{fl/fl}$* mice for more than 3 generations. All mice used for experiments had dark brown or black fur color. All mice used for experiments were between 8 to 12 weeks old.

Conditional gene targeting of *Pak2*. Two similar *Pak2* targeting vectors were designed in our laboratories each with *Pak2* exon 2 flanked by a 5′ *loxP* site and a 3′ *loxP* site (Fig. 1A). A neomycin resistance gene was inserted between two *Frt* sites 3′ to the *Pak2* exon 2 but 5′ to the 3′ *loxP* site. Detailed information about the constructs is available upon request. Embryonic stem (ES) cells were transfected with the targeting vector, selected with neomycin, and genotyped using primers shown in Table S1 in the supplemental material. Targeted ES cells were injected into C57BL/6J blastocysts to produce chimeras, and chimeras were bred to identify mice with germ line transmission of the floxed allele. The neomycin cassette was either removed at this point by crossing the Pak2 floxed mice with B/bSJL.Tg mice or before blastocyst injection by electroporating ES cells with Flp recombinase. The pups were named *Pak2$^{fl/+}$* and crossed with *Tie2-Cre*, *CreER^{T2}*, and *VECadherin-CreER^{T2}* (*VEC-CreER^{T2}*) mice to obtain *Tie2-Cre*; *Pak2$^{fl/wt}$* mice, *CreER^{T2}*; *Pak2$^{fl/wt}$* mice, and *VEC-CreER^{T2}*; *Pak2$^{fl/wt}$* mice. These mice were then crossed with *Pak2$^{fl/wt}$* or *Pak2$^{fl/fl}$* mice to obtain *Tie2-Cre*; *Pak2$^{fl/fl}$* mice, *CreER^{T2}*; *Pak2$^{fl/fl}$* mice, and *VEC-CreER^{T2}*; *Pak2$^{fl/fl}$* mice. The *Pak2$^{fl/fl}$* mice created at Fox Chase Cancer Center and Genentech yielded indistinguishable results.

Histology. Freshly dissected embryos and tissues from adult mice were formalin fixed, embedded in paraffin blocks for sectioning, and mounted onto glass slides. For whole-mount immunostaining, embryos and yolk sacs were fixed in 4% paraformaldehyde, washed with phosphate-buffered saline (PBS) containing 0.1% Triton X-100 (TX100), blocked in PBS containing 0.1% TX100 and 2% bovine serum albumin (BSA), and incubated with unconjugated or fluorescein isothiocyanate (FITC)-conjugated rat anti-CD31, Ki67, or cleaved caspase 3 (see Table S2 in the supplemental material). Yolk sacs were washed extensively and then mounted flat on glass slides in a drop of glycerol and imaged using a Nikon Tie-E fluorescence microscope. At least five embryos were stained and imaged per condition and per genotype.

MLEC isolation and culture. All mice used for mouse lung endothelial cell (MLEC) isolation were culled by cervical dislocation. The lungs were collected immediately and transferred to prechilled 50-ml conical tubes containing 30 ml endothelial cell growth medium (EGM). The lungs were minced for approximately 5 min with sharp scissors in pieces smaller than 1 mm^3 and digested with 1 ml collagenase (1 mg/ml, 37°C, 1 h). Ten milliliters of EGM was added to the digested tissue, and it was pipetted up and down 10 times to separate the cells. The digested tissue was then passed through a cell strainer with 70-μm pores. The individual cell mixture was centrifuged, resuspended in EGM, and plated on fibronectin/collagen-coated plates. Forty-eight hours later, the medium was removed, cells were washed with PBS 3 times, and labeled for EC isolation. EC isolation was performed as previously described (18). Four milliliters of EGM containing 40 μg DilAcLDL (acetylated low-density lipoprotein labeled with 1,1′-dioctadecyl-3,3,3,3′-tetramethyl-indocarbocyanine perchlorate) (Biomedical Technologies) was added to the cells for 4 h at 37°C. The cells were then trypsinized, sorted by fluorescence-activated cell sorting (FACS), and cultured in complete EGM on fibronectin/collagen-coated plates. The cells maintained their characteristics for 5 to 8 passages. MLEC culture plates were coated with 2 ml/100-mm dish of coating solution (collagen I [25 μg/ml], fibronectin [5 μg/ml], and BSA [100 μg/ml] in double-distilled water). The coating solution was spread on the plate, and the plates were incubated at 37°C overnight. The following day, the plates were washed at least 3 times with PBS and stored at 4°C.

To delete the *Pak2* gene, MLECs were treated for 48 h with 1 μM 4-OH-tamoxifen (4-OHTx) and then cultured in medium without 4-OHTx for at least 48 h before being used for assays.

Pooled human umbilical vein endothelial cells (HUVECs) were purchased from Lonza (Walkersville, MD) and cultured in complete EGM2 (Lonza, Walkersville, MD) for a maximum of six passages. HUVECs were transfected with individual SilencerSelect (Life Technologies) Pak2 and nontargeting control (ctl) small interfering RNA (siRNAs) using Lipofectamine RNAiMAX (Life Technologies). siRNA sequences are shown in Table S3 in the supplemental material. Transfected HUVECs were used for experiments 24 to 72 h after transfection.

Immunofluorescence. HUVECs were fixed in 4% paraformaldehyde for 20 min and permeabilized in PBS containing 0.1% Triton X-100 for 5 min. The cells were washed three times with PBS and blocked for 1 h in PBS containing 2% BSA and 0.1% TX100. The cells were incubated with primary antibodies for 1.5 h at 22°C, washed three times with PBS containing 0.1% Triton X-100, and incubated with secondary antibodies for 45 min. The cells were washed extensively with PBS and mounted in Prolong Gold with 4′,6′-diamidino-2-phenylindole (DAPI). Antibody details are provided in Table S2 in the supplemental material.

Embryo body size measurement. Embryo pictures were taken with an Evos microscope at a magnification of ×40. The area corresponding to the whole embryo body was measured using ImageJ software. The highest area value for the embryo body was used for normalization.

Tamoxifen dosing. Eight- to 12-week-old mice received 80 to 100 mg of 4OHTx/kg of body weight by oral gavage for 5 consecutive days. For oral gavage, 4-OHTx was dissolved in ethanol at a concentration of 50 mg/ml and then diluted with corn oil (Sigma) to a final concentration of 10 or 20 mg/ml.

Adenovirus infection of primary MLEC. Adenovirus expressing wild-type Pak2 (WT-Pak2) (Adeno-Pak2) was a generous gift from George E. Davis, University of Missouri. Adenovirus expressing constitutively active Mek (Mek-CA) (Adeno-Mek-CA) was a generous gift from Jun-Ichi Abe, University of Rochester Medical Center. MLECs were infected with Adeno-Pak2 or Adeno-Mek-CA for 12 h and used for experiments 24 to 96 h after infection.

Western blotting. Protein cell lysates were obtained by lysing MLECs in TNE buffer (50 mM Tris-HCl [pH 7.4], 100 mM NaCl, 0.1 mM EDTA, 0.1% Triton X-100) with protease inhibitor cocktail (catalog no. P8340; Sigma). Protein concentration was measured by the Bradford method, and 20 μg total protein was run on a 4 to 20% gradient gel (Bio-Rad). The proteins were then transferred to a nitrocellulose membrane that was blocked in 5% nonfat dry milk. Antibody information is presented in Table S2 in the supplemental material.

Proliferation and apoptosis assays. For the proliferation assay, the MLECs were plated at a concentration of 10^5 cells/ml. The cells were stained with trypan blue and counted every day for 8 consecutive days. For the apoptosis assay, the MLECs were treated with 4OHTx for 4 days and further cultured without 4OHTx for 5 to 8 days. The 4OHTx-treated *CreER^{T2}*; *Pak2$^{wt/wt}$* or *CreER^{T2}*; *Pak2$^{fl/fl}$* MLECs were incubated with Guava Nexin reagent (Millipore) for 30 min following the manufacturer's protocol. Annexin V staining was assessed with a Guava EasyCyte instrument (Millipore).

Adhesion assay. For the adhesion assay, MLECs were plated on E-plates (ACEA Biosciences). E-plates are single-use, disposable devices used for performing cell-based assays on the xCELLigence system. Each individual well on an E-plate incorporates a sensor electrode array that allows cells in the well to be monitored and assayed. E-plates were coated for MLEC cultures as described above. The day of the experiment, MLECs were trypsinized and 5,000 cells were plated in 100 μl EGM. Attachment was assessed as cell index every 15 min with a real-time cell analyzer (RTCA) dual-plate (DP) instrument. Cell index is a measure of both cell

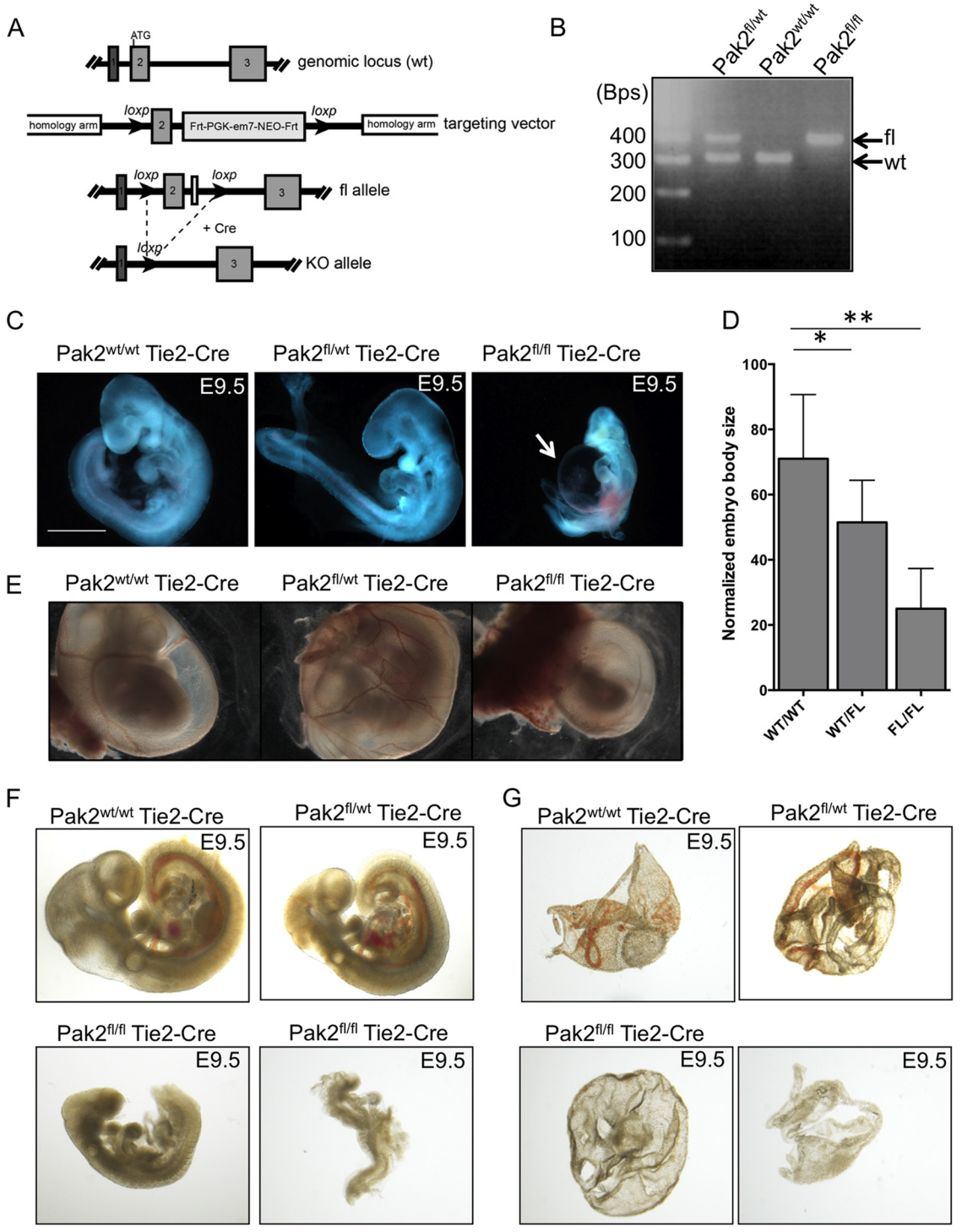

FIG 1 Endothelial deletion of *Pak2* results in embryo lethality. (A) Schematic representation of the targeting strategy used to insert *loxP* sites flanking exon 2 of the *Pak2* gene. (B) Mice were genotyped by PCR. The amplified WT *Pak2* allele is 391 bp, and the amplified *Pak2* FL allele is 306 bp. The positions of molecular size markers (in base pairs) is shown to the left of the gel. (C) On E9.5, embryos were isolated from pregnant dams and immediately imaged. Bar, 1 mm. (D) Embryo body sizes were measured by using ImageJ and normalized to the highest value (WT [$n = 13$], WT/FL [$n = 16$], FL/FL [$n = 9$]). Values are means plus standard deviations (SD) (error bars). Values that are significantly different are indicated by asterisks and bars as follows: *, $P < 0.05$; **, $P < 0.01$. (E) Representative yolk sacs containing embryos at E9.5. (F and G) On E9.5, whole embryos (F) or yolk sacs (G) from WT, WT/FL, FL/FL moderate phenotype, and FL/FL severe phenotype were imaged on a white background for better visualization of vasculature.

number and the surface occupied by each individual cell. The experiments were performed in triplicate and repeated three times.

Migration assay. For the migration assay, MLECs were plated in the top chamber of a CIM-plate (CIM stands for cell invasion/migration). CIM-plates 16 are single-use, disposable devices used for performing cell invasion and cell migration assays on the RTCA DP instrument. The CIM-plate 16 comprises a plate cover (lid), an top chamber, and a bottom chamber. The top chamber has 16 wells that are sealed at the bottom with a microporous polyethylene terephthalate (PET) membrane containing microfabricated gold electrode arrays on the bottom side of the membrane. The median pore size of this membrane is 8 μm. The bottom chamber has 16 wells, each of which serves as a reservoir for medium and any chemoattractant for the cells in the corresponding top chamber wells. MLECs were starved overnight in endothelial basal medium (EBM). The next day, 10,000 cells in 100 μl EBM were added to the top chamber of the CIM-plate. The bottom chamber contained 150 μl EBM with 10% fetal bovine serum. Migration toward serum was monitored as cell index every 30 min for 36 h.

Wound healing assay. MLECs treated with 4OHTx or not treated with 4OHTx were plated to confluence on six-well plates and cultured for 24 h. A scratch was made with a 1-ml pipette tip, the detached cells were removed by washing with warm medium, and then medium was readded to the wells. Pictures of the scratch were taken at different time points over 24 h. The experiment was repeated more than three times, and each time it was performed in triplicate.

HUVECs were transfected with siRNAs and plated to confluence in an Essen ImageLock 96-well plate (Essen BioScience, Ann Arbor, MI) 24 h later. After overnight incubation, the monolayers were wounded with a WoundMaker device (Essen BioSciences, Ann Arbor, MI), and detached cells were removed by gently washing the cells 3 times with warm medium. After the final wash, EBM2 with 0.2% fetal calf serum (FCS) with or without 50 ng/ml vascular endothelial growth factor (VEGF) (R&D Systems, Minneapolis, MN) was added to the wells. Images were collected and quantified every 4 h in an Incucyte microscope (Essen BioScience, Ann Arbor, MI).

Two-dimensional (2D) network formation assay. ECMatrix from angiogenesis assay kit (Millipore) was thawed at 4°C overnight. One hundred microliters of thawed Matrigel was plated per well in a 96-well plate and allowed to solidify at 37°C for 1 h.

A total of 10,000 MLECs were plated per well on the solidified matrix according to the angiogenesis assay kit protocol (Millipore) in 200 μl EGM. HUVECs (10,000/well) were plated on 50 μl of freshly solidified growth factor reduced Matrigel (BD Biosciences) (~30 min, 37°C) in a 96-well plate, and 150 μl EBM2 containing 0.5% FCS supplemented with 50 ng/ml basic fibroblast growth factor (bFGF) (Roche) was added to each well. EC tubes and networks were imaged 8 h (MLECs) or 16 h (HUVECs) after plating and quantified following the guidelines in the angiogenesis assay kit. A numeric value was attributed to the network pattern observed in each well as follows: 5, complex mesh-like structures develop; 4, closed polygons begin to form; 3, sprouting of new capillary tubes visible; 2, capillary tubes visible and no sprouting; 1, cell begin to migrate and align themselves; 0, individual cells that are well separated. Experiments were repeated at least 3 times, in triplicate.

Fibrin bead assay. MLECs and HUVECs were incubated with Cytodex3 beads (19) (Amersham Pharmacia Biotech, Piscataway, NJ) at a concentration of 400 cells/beads. Cells and beads were incubated at 37°C for 4 h with gentle agitation every 20 min. Cell-covered beads were transferred to a 25-cm^2 flask and left at 37°C overnight. The next day, HUVECs were transfected and incubated with siRNAs for 6 h in a 25-cm^2 flask. MLECs and HUVECs were washed 3 times with growth medium and resuspended at a concentration of 200 beads/ml in 2.5 mg/ml fibrinogen (Sigma, St. Louis, MO) with 0.15 U/ml aprotinin (Sigma). Fibrinogen-bead solution (500 μl) was transferred to a well in a 12-well plate, and 0.6 U thrombin was added. The fibrin clot was allowed to solidify for 20 min at 37°C. After the clot solidified, 20,000 human skin fibroblasts were plated on top of the fibrin clot, and 1 ml EC growth medium was added to the clot and incubated overnight at 37°C and 5% CO_2. Fresh complete EGM was added every other day for up to 8 days. Single and time-lapse images were acquired using a Nikon phase-contrast microscope equipped with an environmental chamber. Individual MLEC and HUVEC sprouts were measured with ImageJ software.

Miles assay. A Miles assay was performed to measure endothelial cell permeability (20). *VEC-CreER^{T2}* mice or *VEC-CreER^{T2}*; *Pak2$^{fl/fl}$* or *Pak1* KO mice received intraperitoneal injections with 80 mg/kg 4OHTx daily for 5 consecutive days. There were at least three mice per genotype per experiment. The experiment was repeated 3 times. Two weeks after the first injection, the Miles assay was performed as previously described (20). Specifically, 200 μl of 0.5% solution of Evans blue in sterile PBS solution was injected in the tail veins of 8- to 12-week-old mice. The mice were observed for 30 min after which the mice were sacrificed by cervical dislocation. Representative pictures were taken, and organs of interest were collected in prechilled tubes. One of the lungs from each mouse was collected in EGM and used for EC isolation and confirmation of gene deletion. Pieces from different organs were weighed in separate tubes, and then Evans blue was extracted from these tissues in 500 μl formamide overnight at 55°C. Extracted Evans blue was quantified by measuring absorbance at 600 nm. The data (in nanograms of Evans blue extravasated per milligram of tissue) were plotted.

Aortic ring assay. Mice treated with 4-OHTx were sacrificed by cervical dislocation, and the thoracic aorta was isolated and transferred to ice-cold EGM. The periaortic fibroadipose tissue was carefully removed, and aortic rings with a width of 1 mm were cut and embedded in 150 μl Matrigel. The gel was covered with 1 ml of EGM, and blood vessel sprouting was monitored over a period of 15 days.

***In vitro* permeability assay.** HUVECs and MLECs were plated to confluence for 24 to 48 h on 0.4- or 1-μm Transwell inserts (Millipore) in triplicate on a 24-well plate. Either 40 mg/ml trypan blue and 1.8 mg/ml BSA in HBBS buffer (8 g/liter NaCl, 0.14 g/liter $CaCl_2$, 0.1 g/liter $MgSO_4 \cdot 7H_2O$, 0.4 g/liter KCl, 0.1 g $MgCl_2 \cdot 6H_2O$, 0.06 g/liter KH_2PO_4, 1 g/liter D-glucose, 0.06 g/liter $Na_2HPO_4 \cdot 2H_2O$) or 2 mg/ml FITC-dextran (Sigma) in EGM2 was added to the top chamber of the insert. The absorbance of trypan blue (600 nm) or the fluorescence of FITC-dextran contained in the bottom chamber was measured over or after 60 min.

Statistical analysis. All graphs were created using Prism or Excel software. Statistical analysis was performed using Student's *t* test, and *P* values of <0.05 were considered statistically significant.

Study approval. All studies were done in concordance with protocols approved by the Fox Chase Cancer Center Animal Facility or the Genentech Institutional Animal Care and Use Committee. Mouse colonies maintained at Genentech were housed in a barrier facility, and their care conformed with California state legal and ethical standards of animal care.

RESULTS

Endothelium-specific deletion of Pak2 results in early embryo lethality. Group I Paks are known to modulate vascular signaling in cultured ECs (14, 15, 21) and in multiple animal models (5, 13). In mice, homozygous *Pak2* KO causes embryonic lethality at E8.5 due to multiple development abnormalities, including cardiovascular defects (12). Due to the vascular phenotype observed in the *Pak2* KO mice, we decided to investigate whether *Pak2* is essential in vascular ECs during development. In order to allow temporal and tissue-specific control of the *Pak2* gene, we inserted *loxP* sites flanking the first coding exon (exon 2) of the *Pak2* gene (Fig. 1A). We assessed *Pak2$^{wt/wt}$*, *Pak$^{fl/wt}$*, and *Pak2$^{fl/fl}$* mouse genotypes by using PCR (Fig. 1B; see Table S1 in the supplemental material). *Pak2$^{fl/fl}$* mice were viable, fertile, and indistinguishable from *Pak2$^{fl/+}$* and *Pak2$^{wt/wt}$* mice.

We crossed *Pak2*-floxed mice with the *Tie2-Cre* transgenic mouse line in order to drive recombination at the floxed *Pak2*

allele in ECs. Using Mendelian ratios, we would expect that 25% of pups should have a *Tie2-Cre*; $Pak2^{fl/fl}$ genotype; however, no *Tie2-Cre*; $Pak2^{fl/fl}$ (e*Pak2* KO) pups were observed among >200 pups. This observation strongly suggests that *Pak2* deletion in ECs is embryonic lethal.

Endothelial Pak2 deletion leads to defects in cardiovascular development. To recover *Tie2-Cre*; $Pak2^{fl/fl}$ embryos, we set up timed matings between $Pak2^{fl/fl}$ mice (females) and *Tie2-Cre*; $Pak2^{fl/wt}$ mice (males), harvested embryos at various gestational stages, and used a small yolk sac clipping for genotyping. At E10.5 days postfertilization, we did not observe any e*Pak2* KO embryos ($n = 50$ embryos). At E9.5, embryos containing at least one *Pak2* allele had developed circulation with visible cerebral vascularization as well as a clearly formed dorsal aorta (Fig. 1C and F, top panels). In contrast, all of the e*Pak2* KO embryos showed various levels of growth and developmental retardation and defective vascularization (Fig. 1C and F, bottom panels). Some embryos presented a more moderate phenotype; these embryos were smaller, but the phenotype appeared at a similar gestational age (Fig. 1F, bottom left panel). The embryos with the most severe phenotypes had not turned and displayed an open neural tube and appeared degraded (Fig. 1C, right panel, and F, bottom right panel). e*Pak2* KO embryos displayed various levels of pericardial edema (Fig. 1C, arrow), which is indicative of cardiac dysfunction. *Tie2-Cre*; $Pak2^{fl/wt}$ embryos did not have gross cardiovascular defects, but they were ~25% slightly smaller than *Tie2-Cre*; $Pak2^{wt/wt}$ embryos (Fig. 1D and F, top right panel).

By E9.5, yolk sacs from *Tie2-Cre*; $Pak2^{wt/wt}$ embryos have well-defined blood vessels that branch throughout the sac (Fig. 1E, left panel, and G, top left panel). Similar to the embryo body, the yolk sacs from e*Pak2* KO embryos were pale, and the prominent vitelline vessel and smaller branched vessels were absent (Fig. 1E, right panel, and G, bottom panels).

E9.5 embryos were fixed, sectioned in the sagittal plane, and hematoxylin and eosin (H&E) stained (Fig. 2A). Examination of the developing hearts in these embryos showed areas of a continuous endocardial layer in *Tie2-Cre*; $Pak2^{fl/wt}$ embryos ($n = 11$) and *Tie2-Cre*; $Pak2^{wt/wt}$ embryos ($n = 4$) (Fig. 2A, arrow). In contrast, in e*Pak2* KO hearts, the endocardial layer was not visible or appeared largely disrupted in 85% of the e*Pak2* KO embryos examined ($n = 12$) (Fig. 2A, arrow). In addition, the myocardium appeared impaired with fewer areas of trabecula initiation (Fig. 2A, arrowhead).

To further study the developmental state of blood vessels in e*Pak2* KO embryos, we immunostained whole embryos with a CD31 antibody. *Tie2-Cre*; $Pak2^{wt/wt}$ embryos presented with a well-formed dorsal aorta with distinct intersomitic branches that coalesce to form a complex microcapillary network (Fig. 2B). e*Pak2* KO embryos display a dorsal aorta that branched out into intersomitic blood vessels; however, the intersomitic branches are dilated and shorter and do not form a microcapillary network (Fig. 2B, magnified panels). In sagittal sections of CD31-stained E9.5 e*Pak2* KO embryos, the dorsal aorta presented with areas of collapse and dilation (Fig. 2C). These blood vessels were also devoid of red blood cells (Fig. 2C, magnified panels), explaining our inability to directly visualize the vasculature.

CD31-stained yolk sacs from E9.5 e*Pak2* KO embryos showed severely inhibited vascular remodeling compared to yolk sacs from *Tie2-Cre*; $Pak2^{wt/wt}$ embryos. The yolk sacs from the *Tie2-Cre*; $Pak2^{wt/wt}$ embryos showed remodeled branched vessels interspersed in the surrounding vascular plexus (Fig. 2D). The yolk sac vessels from e*Pak2* KO embryos were dilated compared to blood vessels from *Tie2-Cre*; $Pak2^{wt/wt}$ yolk sacs (Fig. 2E).

In line with our observation that endothelial deletion of *Pak2* is embryonic lethal, e*Pak2* KO sagittal sections showed focal areas of cleaved caspase 3 in embryos with a moderate phenotype and more widespread cleaved caspase 3 immunostaining in embryos with a severe phenotype (Fig. 2F). These areas of increased apoptosis are mirrored by areas of decreased cell proliferation, as measured by Ki67 staining (Fig. 2F).

Pak2 depletion inhibits proliferation and survival of ECs. In order to obtain *Pak2* KO MLECs (mouse lung endothelial cells) for *in vitro* studies, we crossed the $Pak2^{fl/fl}$ mouse with B6.Cg-Tg(Plp1-cre/ESR1)3Pop/J mouse that has a tamoxifen-inducible Cre-mediated recombination system. MLECs were isolated from $CreER^{T2}$; $Pak2^{fl/fl}$ mice, cultured, and treated with 4-OHTx to specifically deplete *Pak2 in vitro* (Fig. 3A). We measured cell proliferation of *Pak2* KO MLECs ($CreER^{T2}$; $Pak2^{fl/fl}$ MLECs with 4-OHTx exposure) and wild-type (WT) MLECs ($CreER^{T2}$; $Pak2^{fl/fl}$ MLECs without 4-OHTx exposure) over 8 days, and trypan blue-stained cells were directly counted. After 8 days, an ~3.5-fold reduction in cell proliferation was observed in *Pak2* KO MLECs compared to control MLECs (Fig. 3A, circles). Similar results were observed in proliferation assays that compared *Pak2* KO MLECs with 4-OHTx-treated $CreER^{T2}$; $Pak2^{wt/wt}$ MLECs (data not shown). Since tamoxifen treatment has been shown to reduce secreted VEGF levels in medium (22), we treated both control and *Pak2* KO MLECs with saturating levels of VEGF. As expected, we observed a VEGF-dependent increase in the growth of control MLECs, while the *Pak2* KO MLECs still exhibited an ~3.5-fold reduction in cell number (Fig. 3A, squares). Similar results were also observed in proliferation assays with HUVECs transfected with Pak2-specific siRNAs, which showed a 2- to 3-fold reduction in cell proliferation (Fig. 3B).

Next, we determined whether Pak2 deletion induces apoptosis in MLECs. *Pak2* KO MLECs showed an ~5-fold increase in annexin V staining relative to control MLECs, indicating that Pak2 depletion results in an increase in apoptosis (Fig. 3C). Consistent with this finding, *Pak2* KO MLECs showed decreased levels of anti-apoptotic Bcl2 and increased cleaved caspase 3 levels (Fig. 3C, right panels). We next tested whether *Pak2* KO in MLECs affects cell cycle progression. *Pak2* KO in MLECs did not affect the percentage of G_2/M- and S-phase cells, suggesting that Pak2 does not significantly regulate progression through the cell cycle (data not shown).

Pak2-deficient ECs have impaired adhesion and migration. EC attachment and migration are essential events for angiogenesis (23), and several members of the Pak family have been reported to regulate these processes in a variety of cell types (14, 24). Due to these previous observations and to the fact that Pak2 depletion leads to an increase in apoptosis in MLECs (Fig. 3C), we investigated whether depletion of *Pak2* affects EC adhesion and migration. WT MLECs and *Pak2* KO MLECs were plated on E-plates, and the cell index was monitored in a xCELLigence system (Fig. 3D). At early time points, *Pak2* KO MLECs had a smaller cell index than WT MLECs did, suggesting deficient attachment. *Pak2* KO cells reached the same cell index as WT cells did 6 h after plating but fell behind again after 24 h (Fig. 3D, top panel). Since the cell index is also a measure of cell number, it is possible that the smaller cell index of *Pak2* KO MLECs at time points later than 48 h is due to slower proliferation of *Pak2* KO MLECs (Fig. 3A).

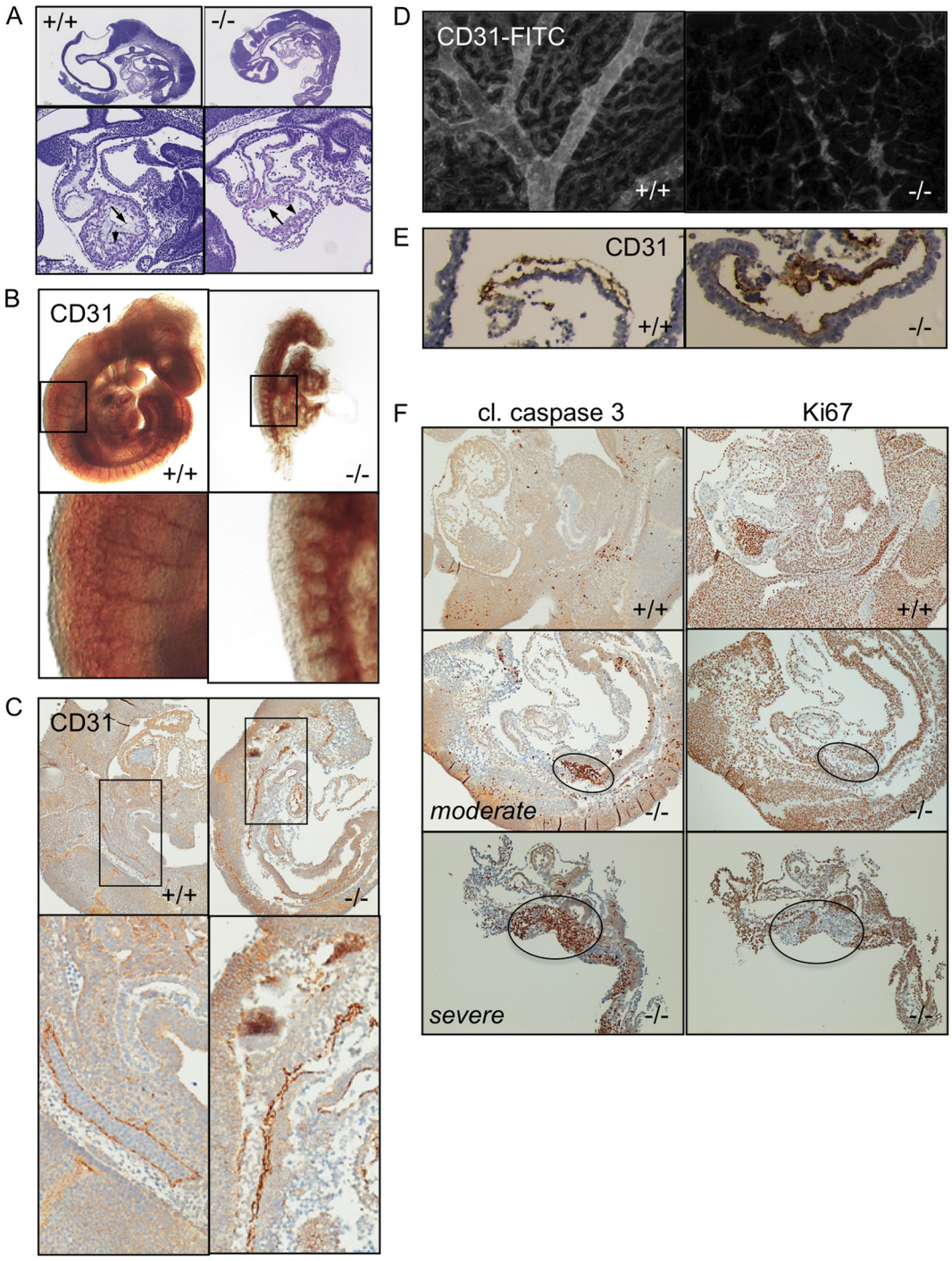

FIG 2 Endothelial *Pak2* KO embryos and yolk sacs have abnormal vasculature. (A) H&E-stained sagittal sections of E9.5 embryos. Magnified regions show the developing heart. (B) Whole-mount CD31 immunohistochemistry (IHC) of E9.5 embryos. The magnified panels show morphology of intersegmental vessels. (C) CD31 IHC of sagittal sections of E9.5 embryo. Magnified panels show regions of the dorsal aorta. (D) Whole-mount CD31 immunofluorescence (IF) of yolk sacs from E9.5 embryos. (E) CD31 IHC of sectioned yolk sacs from E9.5 embryos. (F) Cleaved (cl.) caspase 3 and Ki67 IHC of E9.5 embryos. Two representative examples of e*Pak2* KO embryos show the typical variation observed at this gestational stage. Circled areas indicate increased apoptosis (left panels) and decreased cell proliferation (right panels).

Interestingly, when MLECs were plated on electrodes that have not been previously coated with fibronectin/collagen, *Pak2* KO cells had a lower cell index at all time points compared to WT MLECs (Fig. 3D, bottom panel). This suggests that for attachment purposes, *Pak2* deletion can be partially overcome in the presence of an extracellular matrix, but *Pak2* is essential in its absence.

Next, we determined whether depletion of *Pak2* affects endothelial motility using chemotaxis and wound healing assays. First,

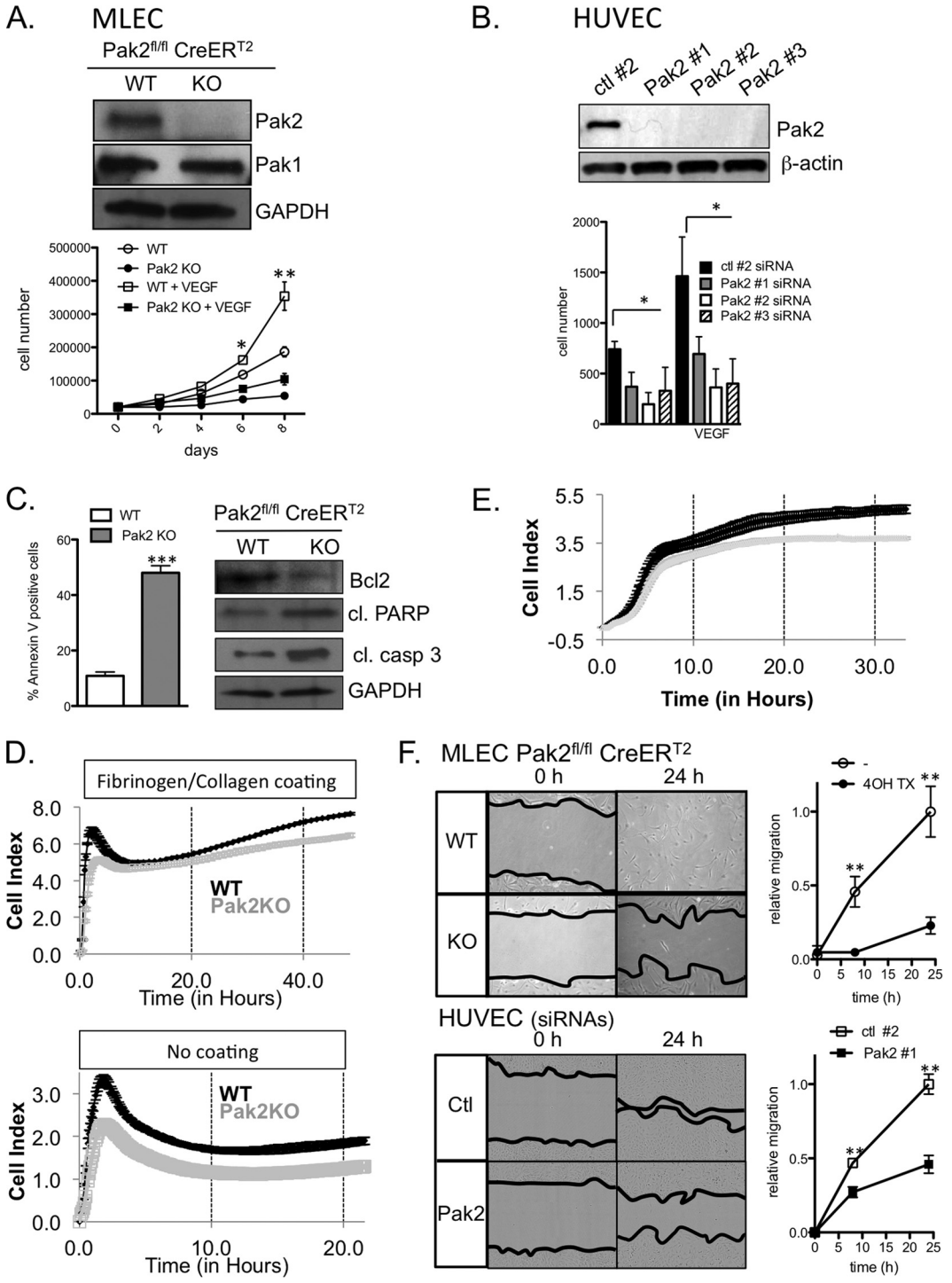

FIG 3 *Pak2* KO and KD inhibit proliferation, attachment, and migration of ECs and enhance apoptosis. (A) Proliferation of MLECs in the presence and absence of VEGF. Western blot analysis of Pak1 and Pak2 expression in *CreER*^{T2}; *Pak2*$^{fl/fl}$ MLECs treated with vehicle and 4-OHTx. GAPDH, glyceraldehyde-3-phosphate dehydrogenase. (B) Proliferation of HUVECs transfected with control (ctl) short hairpin RNA (shRNA) or three different Pak2 shRNAs. The results of Western blot analysis of Pak2 expression are shown. (C) Apoptosis analysis of *CreER*^{T2}; *Pak2*$^{fl/fl}$ MLECs treated with vehicle and 4-OHTx. (Left) Percentage of annexin V-positive MLECs. (Right) Western blot analysis of apoptosis markers Bcl2, cleaved procyclic acidic repetitive protein (PARP), and cleaved caspase 3 from MLEC lysates. (D) Long-term cell attachment assay with MLECs on fibronectin/collagen-coated or noncoated plates. (E) Chemotactic migration of MLECs toward 10% serum. (F) Wound healing assay using MLECs and HUVECs. Images show the initial wound width and wound closure after 24 h. Relative wound migration was quantified from images at 0, 8, and 24 h. Error bars represent SD in all panels. Experiments were repeated more than 4 times. Symbols: *, $P < 0.05$; **, $P < 0.01$; ***, $P < 0.001$.

we assessed the role of Pak2 in chemotactic migration toward 10% serum. WT MLECs and *Pak2* KO MLECs were plated on CIM-16 plates. Medium containing 10% serum or vehicle was added to the bottom chamber, and the cell index was monitored for 33 h in a xCELLigence system. We observed a significant reduction in the rate of chemotactic migration toward 10% serum (Fig. 3E). In wound healing migration assays, a uniform scratch was introduced into MLEC and HUVEC monolayers, and closure of the wound was monitored at different time points using a phase-contrast microscope (0- and 24-h time points shown in Fig. 3F). *Pak2* KO MLECs and Pak2 knockdown (KD) HUVECs showed considerably lower directional migration rates compared to those of WT MLECs and HUVECs transfected with control siRNA, and this resulted in an inability to close the wounded area in 24 h (Fig. 3F). Together, these data indicate that endothelial Pak2 is critical for efficient cell migration.

Sprouting and lumen formation are inhibited in Pak2-depleted ECs. We performed a simple 2D tubule formation assay on Matrigel. MLECs (top panels) and HUVECs (bottom panels) were plated on top of Matrigel and imaged after 8 and 16 h, respectively (Fig. 4A). WT MLECs and HUVECs transfected with control siRNAs aligned, sprouted, and formed interconnected networks. Similarly, *Pak1* KO MLECs were able to form complex network structures, indistinguishable from WT ECs. *Pak2* deletion resulted in a reduction in tubule formation (2.5-fold in MLECs and 2-fold in HUVECs). We also observed a severe reduction in tubule formation in HUVECs treated with a pan-Pak inhibitor (data not shown). Expression of exogenous Pak2 in MLECs partially restored tubule formation in *Pak2* KO MLECs (Fig. 4A).

Next, we used a three-dimensional (3D) *in vitro* angiogenesis assay that recapitulates several processes required for *in vivo* angiogenesis, including cell proliferation, extracellular matrix (ECM) digestion/remodeling, migration, branch formation, lumen formation, and anastomization (25). MLEC- and HUVEC-covered Cytodex3 beads were embedded in a fibrin clot and monitored for 5 to 8 days. We observed robust sprout and lumen formation with WT MLECs and HUVECs transfected with control siRNAs (Fig. 4B), and *Pak1* KO MLECs sprouted and formed tubules similar to WT MLECs. *Pak2* KO and KD in ECs robustly inhibited sprout formation. The number of sprouts per bead was reduced 2.3-fold in *Pak2* KO MLECs and 3-fold in Pak2 KD HUVECs, and the sprout length was reduced 5.1-fold in *Pak2* KO MLECs and 2.5-fold in Pak2 KD HUVECs. Importantly, infection of *Pak2* KO MLECs with Pak2-expressing adenovirus partially restored sprout formation (Fig. 4B). From time-lapse images of sprout formation, it appears that Pak2 KD inhibits sprouting early in the sprout initiation phase, and only a few cellular protrusions are observed in the surrounding matrix (see Movie S1 in the supplemental material).

Last, we tested angiogenesis *ex vivo* in an aortic ring assay. For this assay, 1-mm-wide rings of thoracic aorta from *CreER*^{T2}*Pak2*$^{wt/wt}$, *CreER*^{T2}; *Pak2*$^{fl/fl}$, and *Pak1* KO mice treated with 4-OHTx were embedded in Matrigel and monitored for 15 days. Endothelial cells lining aortic rings from *CreER*^{T2} *Pak2*$^{wt/wt}$ mice sprouted and formed tube-like structures resembling primordial blood vessels (Fig. 4C, left magnified panel). We observed robust inhibition of microvessel growth from the Pak2-depleted aortas compared to the control aortas. *Pak1* KO aortic rings gave rise to a microvessel network comparable to control aortic rings (Fig. 4C, middle panels). Together, these data provide further support that Pak2, but not Pak1, is critical for angiogenesis.

Pak2 expression is required for endothelial barrier maintenance. The vascular endothelium serves a critical function as a semipermeable barrier between the intra- and extravascular space, and Pak proteins have been previously reported to modulate this barrier function (5, 15). We investigated whether Pak2 contributes to endothelial barrier integrity in an *in vitro* permeability assay. MLECs and HUVECs were plated to confluence on 1- and 0.4-μm Transwell inserts, respectively. After establishing cell-cell junctions, we measured the amount of trypan blue-BSA (MLECs) or FITC-dextran (HUVECs) that extravasated to the opposite side of the cell monolayer. At 60 min, Pak2 KO and KD resulted in an ~2-fold increase in MLEC and HUVEC permeability, indicating that Pak2 is required for endothelial barrier integrity. Expression of exogenous Pak2 in MLECs partially restored endothelial monolayer barrier function (Fig. 5A).

In order to test vascular permeability *in vivo*, we used *VEC-CreER*^{T2}; *Pak2*$^{fl/fl}$ mice that express *CreER*^{T2} under the endothelium-specific *VEC* promoter. We treated *VEC-CreER*^{T2}; *Pak2*$^{fl/fl}$, *VEC-CreER*^{T2}; *Pak2*$^{wt/wt}$, and *Pak1* KO mice with 4-OHTx for 5 consecutive days. Nine days later, Evans blue solution was injected into the tail vein, and extravasation of Evans blue into the interstitial tissue was monitored and quantified 30 min following injection. In *VEC-CreER*^{T}; *Pak2*$^{fl/fl}$ mice treated with 4-OHTx (e*Pak2* KO), we observed an ~3-fold increase in vascular permeability in the lung and skin compared to similarly treated *VEC-CreER*^{T2}; *Pak2*$^{wt/wt}$ and *Pak1* KO mice (Fig. 5B and C). Ubiquitous Pak2 deletion in *CreER*^{T2}; *Pak2*$^{fl/fl}$ also resulted in more permeable endothelium (data not shown). Importantly, ubiquitous Pak2 deletion led to adult mouse lethality 40 days (100 mg/kg Tx) or 20 days (200 mg/kg Tx) upon induction of gene deletion (Fig. 4D).

Pak2 regulates cytoskeletal organization and remodeling in ECs. Next, we investigated potential downstream processes regulated by Pak2 in ECs. First, we examined Pak2's role in regulating the cytoskeleton due to the results we observed in our migration, sprouting, and permeability assays and the well-known role of the Pak kinase family in regulating a number of cytoskeleton-associated proteins (7, 26–28). HUVECs were sparsely and densely plated on fibronectin-coated coverslips and then labeled them with phalloidin, VE-cadherin (VEC) (confluent cells), or phosphorylated myosin light chain (pMLC) antibodies. Sparse control siRNA-transfected HUVECs typically displayed a prominent lamellipodium (Fig. 6A, white arrows), a distinguishable cell polarity, and few stress fibers. The pMLC signal was typically observed at the sides and back of the cells (Fig. 6B, arrows), with few cells with centrally localized pMLC (Fig. 6B, asterisks). In contrast, Pak2 KD HUVECs showed reduced lamellipodial phalloidin staining, an unpolarized morphology, and prominent stress fibers traversing the cell (Fig. 6A) that also stained positive for pMLC (Fig. 6B). In confluent cells, control HUVECs established tight cell junctions containing VEC (Fig. 6C), and actin fibers localized predominantly at the cell periphery (Fig. 6D). Confluent monolayers of HUVECs with Pak2 KD also formed cell-cell contacts, albeit with a more disorganized pattern (Fig. 6C), but showed an increase in robust stress fibers that typically traversed the entire cell length (Fig. 6D). A similar reorganization of stress fibers was observed in HUVECs treated with a pan-Pak inhibitor (data not shown). These data indicate that Pak2 is required for maintaining normal actomyosin localization in sparse and confluent cells, which may contribute to the reduced motility and endothelial barrier integrity we observe in *Pak2* KO and KD ECs. To further

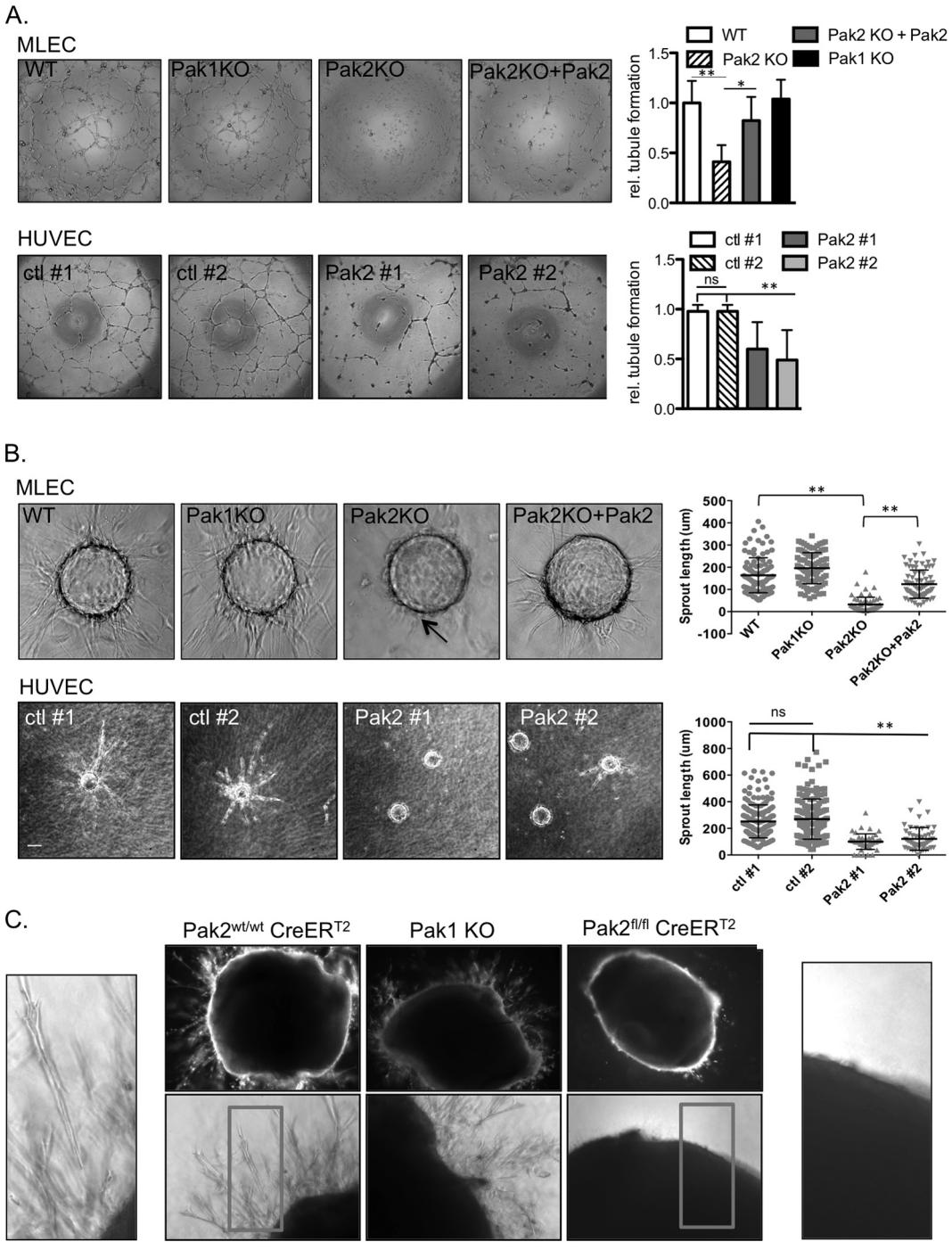

FIG 4 Pak2 KO and KD ECs have impaired angiogenic potential. (A) MLECs and HUVECs were plated on a 2D Matrigel ECM and incubated for up to 16 h. Tubule networks were quantified from phase-contrast images from at least three experiments. rel., relative. (B) MLECs and HUVECs were attached to Cytodex3 beads and embedded in a 3D fibrin gel. Sprout length was measured for MLECs and HUVECs (15 to 17 beads/condition from two independent experiments) after 3 and 8 days, respectively. Each symbol in the scatter plot is a single sprout length. Exogenously expressed Pak2 was introduced in *Pak2* KO MLECs using adenovirus transduction. (C) Aortic ECs sprouting from aortas isolated from 4-OHTx-treated *CreER*^{T2}; *Pak2*$^{wt/wt}$, *CreER*^{T2}; *Pak2*$^{fl/fl}$, and *Pak1* KO mice. Aortas were embedded in a Matrigel ECM and imaged after 15 days. Experiments were repeated at least three times. Error bars represent SD. Symbols: *, $P < 0.05$, **, $P < 0.01$. ns, not significant.

investigate the cause of increased permeability, we analyzed the effect of Pak2 downregulation on adherens junctions by measuring the levels and activity of integrin beta1. We did not observe any difference in the level or activity of integrin beta1 as measured by Western blot and FACS analysis (data not shown).

Next, we determined whether Pak2 regulates actin filament remodeling using forskolin, a cyclic AMP (cAMP)-elevating agent that induces cortical actin assembly and increases endothelial barrier integrity (29). For these experiments, we stimulated confluent HUVECs with vehicle control or forskolin for 20 min and then

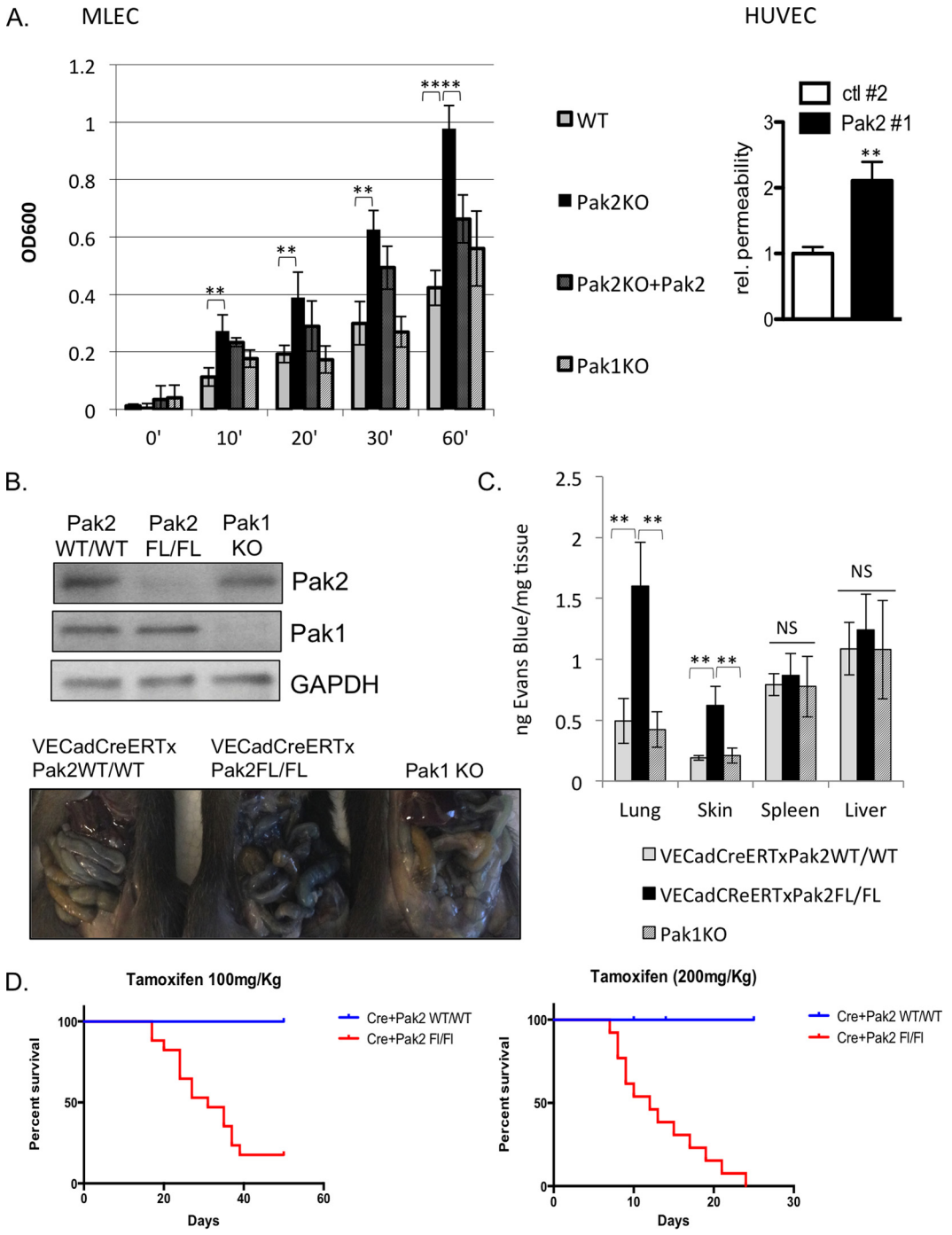

FIG 5 Pak2 is required for endothelial barrier maintenance. (A) MLECs and HUVECs were plated to confluence on 1- or 0.4-μm Transwell filters. Trypan blue-BSA or FITC-dextran was added to the top well, and the amount of trypan blue-BSA or FITC-dextran in the bottom chamber was measured over 60 min (60′). Exogenous Pak2 was expressed by transducing MLECs with Pak2-expressing adenovirus. OD600, optical density at 600 nm. (B) *In vivo* permeability assay in *VEC-CreER*^{T2}; *Pak2*$^{fl/fl}$, *VEC-CreER*^{T2}, and *Pak1* KO mice. Western blot shows deletion of *Pak2* and *Pak1* in corresponding MLECs. (C) Evans blue dye was injected in the tail veins of *VEC-CreER*^{T2}; *Pak2*$^{fl/fl}$, *VEC-CreER*^{T2}, and *Pak1* KO mice that were dosed with 4-OHTx. Evans blue dye was injected into mice, and the dye was extracted with formamide. The amount of extravasated dye was normalized to the tissue mass (in nanograms of Evans blue per milligram of tissue). Error bars represent SD. Experiments were repeated at least three times. **, $P < 0.01$; NS, not significant. (D) Survival curve for *CreER*^{T2}; *Pak2*$^{fl/fl}$ or *CreER*^{T2}; *Pak2*$^{wt/wt}$ mice dosed with 100 mg/kg or 200 mg/kg 4-OHTx.

stained the cells with phalloidin, β-catenin, and Pak2 antibodies. In HUVECs transfected with control siRNA and treated with forskolin, we observed an increase in β-catenin and F-actin organization into a narrow band at cell-cell junctions (Fig. 6E). In HUVECs treated with vehicle control, Pak2 localized to the cytoplasm and punctate structures that localized at the cell periphery. Stimulation with forskolin induced an increase in Pak2 localization at cell-cell junctions (Fig. 6E). The nuclear

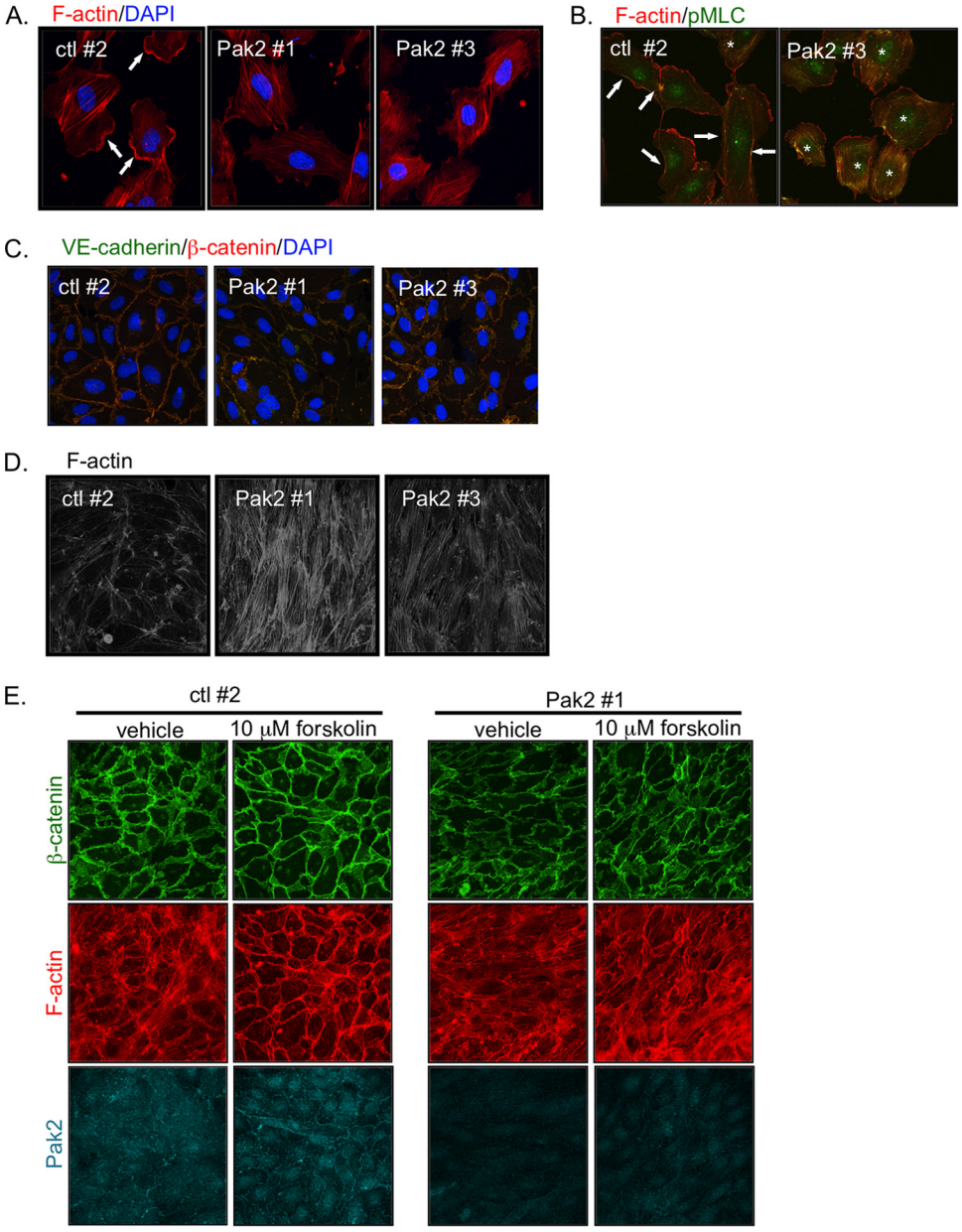

FIG 6 Pak2 regulates cytoskeletal organization and remodeling. (A) HUVECs were sparsely plated on fibronectin-coated slides, fixed, and stained with phalloidin and DAPI. (B) Sparsely plated HUVECs were fixed and stained with pMLC antibody and phalloidin. Arrows indicate phosphorylated myosin light chain (pMLC) enrichment at the sides and back of the cell, and asterisks indicate cells with abundant centrally localized pMLC signal. (C) HUVECs were plated to confluence on fibronectin-coated slides, fixed, and stained with DAPI and VEC and β-catenin antibodies. (D) Confluent HUVECs fixed and stained with phalloidin. (E) HUVECs were plated to confluence, allowed to form cell-cell junctions, stimulated with vehicle control or 10 μM forskolin for 20 min, fixed, and stained with phalloidin and Pak2 and β-catenin antibodies. Images are representative of three independent experiments.

staining with Pak2 antibodies is likely unspecific background as this is observed in control and Pak2 KD cells (Fig. 6E, right bottom panels). In contrast to control HUVECs, Pak2 KD HUVECs showed reduced cortical F-actin and β-catenin remodeling, and most cells still contained abundant central stress fibers (Fig. 6E). These data show that Pak2 increases its junctional localization and modulates cortical F-actin remodeling in the presence of a barrier-enhancing stimulus.

Pak2 signals through the Bmk1/Erk5 pathway. Pak proteins have been previously implicated in angiogenesis and maintaining a healthy endothelial barrier by modulating the MAPK pathway and several molecules involved in the cell contractile mechanism (10, 14, 30). While the role of Pak in angiogenesis has been well established, currently, there is no consensus yet on Pak's role in endothelial permeability. After an in-depth research of vascular-system-related phenotypes of different KO animals, we observed that *Bmk1*/*Erk5* KO mice and endothelial *Bmk1*/*Erk5* KO mice have phenotypes similar to those of *Pak2* KO and endothelial *Pak2* KO mice (31, 32). We therefore hypothesized that in ECs, Pak2 and Bmk1/Erk5 share a signaling pathway.

We studied activation of the *Bmk1/Erk5* pathway in *Pak2* KO ECs. *Pak2* KO MLECs showed markedly lower levels of phosphorylated Bmk1 (P-Bmk1)/Erk5 upon EGF stimulation. These levels were partly restored in *Pak2* KO MLECs that have been previously infected with Pak2-expressing adenovirus. Interestingly, phosphorylated Erk1/2 (P-Erk1/2) levels were not significantly affected in *Pak*2 KO or *Pak*1 KO MLECs, suggesting that Erk1/2 might not be critical in Pak signaling in ECs (Fig. 7A).

To assess whether Pak2-induced events are mediated through Mek5/Erk5 signaling in ECs, we overexpressed constitutively active (CA) Mek5, the upstream activator of Bmk1/Erk5, in *Pak2* KO MLECs. P-Bmk1/Erk5 levels were restored in *Pak*2 KO MLECs infected with CA Mek5-expressing adenovirus (Fig. 7A, Pak2KO+ Mek5 lanes). Restoring P-Bmk1/Erk5 levels by CA Mek5 overexpression resulted in partial protection from apoptosis in *Pak2* KO cells (Fig. 7B and C). Furthermore, *Pak2* KO MLECs infected with CA Mek5 adenovirus were able to heal the wound better in a scratch assay than *Pak2* KO MLECs were (Fig. 7D). Angiogenesis, as measured by a 2D network assay, was also partially restored in *Pak2* KO MLECs that overexpress CA Mek5 (Fig. 7E). Similarly, primary MLECs treated with Frax1036 Pak inhibitor (33) show decreased levels of P-Bmk1/Erk5. Similar to the results obtained in *Pak*2 KO MLECs, overexpression of Mek5CA partially rescued apoptosis in MLECs treated with a small-molecule inhibitor of group I Paks (Fig. 7F). These data suggest that, in ECs, Pak2-mediated cellular events involve signaling through the Bmk1/Erk5 pathway.

DISCUSSION

In this study, we used Cre-expressing mouse models to delete *Pak2* in ECs during development (*Tie2-Cre*) and in the adult (*VEC-CreER^{T2}*). We identified Pak2 as a critical regulator of EC function that ultimately controls vascular morphogenesis in the developing embryo and vessel barrier maintenance in the adult animal.

Due to its well-known role in cell motility, Paks have been posited to play a significant role in angiogenesis. Early studies by Kiosses et al. showed that a Pak inhibitory peptide inhibited angiogenesis in a chick chorioallantoic assay (34). Later genetic studies showed that *Pak2* KO embryos displayed early lethality and vascular defects, implicating this specific group I Pak member as an important regulator in vascular function (12). In this study, we show that specific deletion of *Pak2* in vascular tissues is associated with major defects in angiogenic remodeling and cardiac development and with lethality at E9.5. In contrast to these findings, previous studies showed that deletion of either *Pak1* or *Pak3* is tolerated, and mice lacking either of these genes do not display significant vascular defects (12). These results are consistent with the fact that Pak2 is the main isoform expressed in ECs (35) and the idea that Pak1 and Pak2 have distinct and often opposing roles in mediating various cellular events, as has been suggested by a number of recent studies (36–38).

In vitro analysis of *Pak2* KO MLECs and KD HUVECs demonstrated that this group I Pak modulates several cellular processes that are required during angiogenesis, such as cell migration, sprouting, and proliferation. Previous reports showed that Pak2 and the group II Pak, Pak4, each play a role in endothelial lumen formation in a 3D collagen matrix (24). In our sprouting assay, we show that Pak2 regulates early steps during sprout initiation, such as migration and invasion, which precede lumen formation.

It is probable that the angiogenesis defects are a result of the severe apoptotic events induced by *Pak2* deletion (Fig. 4C and 7C). The role of Pak2 in protecting from apoptosis has been previously documented in various cell lines (39–42). In primary MLECs, expression of constitutively active Mek1 or Mkk4 was not able to rescue apoptosis or angiogenesis defects initiated by *Pak2* deletion (data not shown). However, overexpression of constitutively active Mek5 was partially effective in rescuing *Pak2* KO MLECs from apoptosis, suggesting that in endothelial cells, Pak2 uses multiple pathways to protect against apoptotic events.

Deletion of *Pak2* in ECs induces cytoskeleton modifications similar to those found in ECs deleted for certain upstream regulators or downstream effectors of Pak kinases (24, 43, 44). Indeed, similar to our observations on endothelial *Pak2* KO, endothelial *Rac1* KO, and endothelial *Erk1/2* KO embryos present with severe growth retardation, *Erk1* KO and *Rac1* KO ECs have decreased angiogenic potential, similar to our findings with *Pak2* KO ECs. However, both *Erk*1 KO and *Rac1* KO ECs are associated with a densely packed endothelium that is less permeable to proteins (43, 44).

Vascular barrier integrity is a reversible and dynamic process that is essential for tissue homeostasis, and defects in barrier maintenance and stabilization can result in increased inflammation, edema, and hemorrhage. The roles of Paks in the control of vascular permeability are complex and contingent on the choice of model system, context, and permeability-inducing stimulus (5, 6, 9, 14, 24).

For example, using a peptide inhibitor, Stockton et al. showed that blocking group I Pak activation prevented an increase in permeability across the cell monolayer in response to a wide variety of permeability factors (4). In these studies, a Pak leads to an increase in pMLC in ECs, resulting in contracted ECs that lose contact with the neighboring cells resulting in a more permeable endothelium (4, 7, 45). The Pak2 KD and KO phenotypes we observed, such as an increase in central pMLC-decorated filaments, radial stress fibers, and permeability, seem inconsistent with these potential mechanisms. In further support of a potential propermeability role of Pak2, it has been shown that a Pak inhibitory peptide caused a decrease in lipopolysaccharide (LPS)-induced endothelial permeability in a mouse model of lung inflammation (46). These results suggest that group I Paks play a positive role in promoting permeability. One potential mechanism underlying this model is the phosphorylation of VE-cadherin by Pak2 at S665, an event that promotes the internalization of this cadherin, destabilization of cell junctions, and an increase in *in vitro* monolayer permeability (19).

In contrast to these reports, several studies implicate Pak signaling as a positive regulator of endothelial barrier integrity and recovery in the presence of permeability-increasing stimuli, such as LPS, thrombin, and tumor necrosis factor alpha (TNF-α) (47). Here, Pak activation is proposed to occur downstream of Rap1 signaling, a pathway that protects endothelial junctions by stabilizing junctions and promoting cytoskeletal rearrangements via the cAMP-regulated RapGEF Epac1 (47). We show that Pak2 KD reduced circumferential actin band formation and prevented complete dissolution of stress fibers in the presence of elevated cAMP. In line with Pak's role in promoting endothelial stabilization, it has also been shown that activation of Pak in a hypoxia-induced neonatal pulmonary hypertension mouse model leads to reduction in vascular permeability (13). Further, it has been shown that loss of *pak2a* in a zebrafish model is associated with

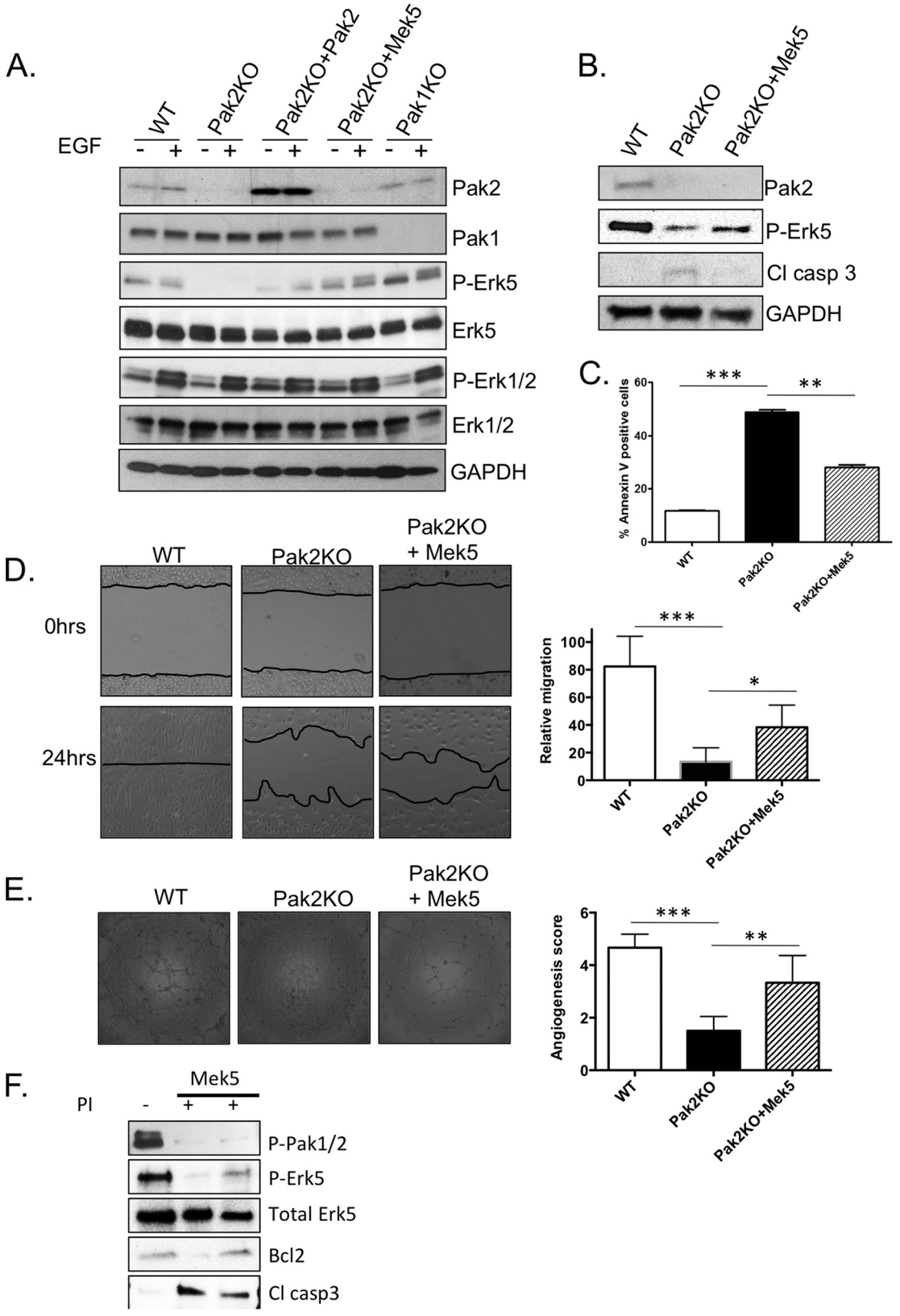

FIG 7 Pak2 regulates the Mek5/Erk5 signaling pathway. (A) Western blot analysis of MLEC protein lysates. MLECs were infected with adenovirus expressing WT-Pak2 and CA-Mek5 for 24 h and then treated with 4-OHTx. The cells were serum starved for 24 h and then induced with 10 ng/ml EGF (+) for 10 min. (B) Western blot analysis of apoptosis markers in protein lysates from MLEC cells infected with CA-Mek5. (C) Apoptosis assay showing percent annexin V-positive MLECs. (D) Wound healing assay with WT, *Pak2* KO, and CA-Mek5 reconstituted MLECs. Error bars represent SD. (E) Tubule network assay with WT, *Pak2* KO, and CA-Mek5 reconstituted MLECs. At least five different fields were given an angiogenesis score according to the manufacturer's recommendation. Error bars represent SD. Symbols: *, $P < 0.05$; **, $P < 0.01$; ***, $P < 0.001$. (F) WT MLECs and MLECs overexpressing constitutively active Mek5 were treated with Frax1036 pan-PakI inhibitor (PI) for 6 h. Western blot analysis of P-Erk5 and apoptosis markers shows that inhibition of Pak1 to Pak3 results in decreased active Erk5 and that Mek5 can partially rescue apoptosis events due to Pak2 loss.

cerebral hemorrhage and increased blood vessel permeability without significantly altering vascular patterning (5, 48). These studies suggest a role for group I Paks, and perhaps Pak2 in particular, in inhibiting vascular permeability. Our studies support this position, as we show that, while loss of *Pak1* has little effect on either endothelial permeability *in vitro* or vascular permeability *in vivo*, reduction or deletion of *Pak2* profoundly increases vascular permeability both *in vitro* and *in vivo* in the lungs and skin of e*Pak2* KO mice. We did not observe an increase in permeability in spleen and liver. This organ-specific increase could be due to better *Pak2* recombination in lung and skin ECs, a more prominent role of Pak2 in ECs from these tissues, or an increase in the susceptibility of these vessels to leak. These organs also presented with a higher Evans blue extravasation in wild-type mice as well, possibly due to the open circulation in hepatic and spleen sinusoidal vessels. Our genetic data thus fall squarely into the camp that posits that Pak2 inhibits EC permeability. As our approach is the first to test the absolute absence of Pak2 in ECs, it is possible that the contradictory permeability results from the literature are due to a necessity of a certain minimum Pak2 threshold level. Possibly, when minimal Pak2 is present in ECs, it can still rescue from apoptosis, maintain the EC barrier function, and initiate an overactivation of Rac signaling that might lead to increased contractility.

To further explain the increased permeability of *Pak2* KO endothelium, we compared various mouse phenotypes that also presented with an increased vascular permeability to the endothelial *Pak2* KO mouse phenotype. Endothelial *Bmk1*/*Erk5* KO embryos and adult *Bmk1*/*Erk5* KO mice have phenotypes that are very similar to those of endothelial *Pak2* KO embryos and mice. Endothelial deletion of *Pak2* leads to embryo lethality at E9.5, while endothelial deletion of *Erk5* is lethal at E10.5. Genetic deletion of *Pak2* has been shown to lead to reduced HSPC (hematopoietic stem and progenitor cell) bone marrow homing and engraftment (36), hinting toward complex roles of Pak2 in various blood cell lineages. It is thus possible that the earlier embryo lethality seen in e*Pak2* KO embryos is due to a more comprehensive signaling, one that partially superimposes Bmk1/Erk5 networks (Fig. 7). Similar to endothelial *Bmk1*/*Erk5* KO embryos, endothelial *Pak2* KO embryos show dilated blood vessels in the embryo body and yolk sac. Furthermore, similar to *Erk5* KO blood vessels, *Pak2* KO blood vessels are more permeable and show impaired angiogenesis. Reports linking Erk5 to angiogenesis are abundant; however, the role Erk5 plays in angiogenic processes seems to vary greatly between different cell and animal model contexts, as well as with various angiogenic stimuli (31, 49, 50). We have found that in a *Pak2* KO context, ECs can be rescued from apoptosis by overexpression of Mek5. Similarly, Pi et al. show that Mek5 can rescue EC apoptosis through a Bad phosphorylation event (51).

Molecular analysis of *Pak2* KO ECs showed decreased levels of P-Erk5 upon induction with EGF. Interestingly, P-Erk1/2 levels were not affected in *Pak1* KO or *Pak2* KO primary ECs, suggesting a selective, and hitherto undetected, link between Pak2 and the Bmk1/Erk5 MAPK pathway. It has been previously shown that Erk5 downregulation in hepatic stellate cells results in decreased Pak phosphorylation (52). In contrast, Komaravolu et al. recently reported that activation of the Bmk1/Erk5 pathway in ECs leads to decreased Pak1 expression both at the mRNA and protein levels (53). Our data support a role for Pak2 upstream of Erk5 and suggest that this pathway is critical for migration, angiogenesis, and protection from apoptosis. In this setting, the reported effects of Erk5 on Pak activity and/or expression may represent a form of feedback regulation, as is common in signaling pathways. Similar to *Erk5*/*Bmk1* KO mice, *Pak2* KO mice die upon induction of gene deletion (Fig. 5D). The adult lethality induced by *Pak2* deletion and the severe phenotypes induced by the endothelial Pak2 deletion raise important warning signs for the use of Pak inhibitors as chemotherapeutic drugs.

These data point to Pak2 as the main group I Pak isoform responsible for maintenance of normal endothelial biology, both during embryonic development and during adulthood.

ACKNOWLEDGMENTS

We thank Luisa Iruela-Arispe for providing the *VEC-CreER*^{T2} mice, Jun-Ichi Abe for adenovirus expressing constitutively active Mek5, the Transgenic Facility and the Lab Animal Facility at the Fox Chase Cancer Center and Genentech for assistance with production of *Pak2*$^{fl/fl}$ mice, the Imaging Facility at the Fox Chase Cancer Center and the Center for Advanced Light Microscopy at Genentech for assistance with immunofluorescence experiments, and Ailey Crow for assistance with actin stress fiber quantification.

This work was supported by grants from the NIH (R01 CA148805 and R01 CA098830), Department of Defense (NF130108), and Children's Tumor Foundation to Jonathan Chernoff, NIH CORE Grant CA06927, and an appropriation from the state of Pennsylvania to the Fox Chase Cancer Center.

REFERENCES

1. **Teo M, Manser E, Lim L.** 1995. Identification and molecular cloning of a p21cdc42/rac1-activated serine/threonine kinase that is rapidly activated by thrombin in platelets. J Biol Chem **270:**26690–26697. http://dx.doi.org/10.1074/jbc.270.44.26690.
2. **Manser E, Leung T, Salihuddin H, Zhao ZS, Lim L.** 1994. A brain serine/threonine protein kinase activated by Cdc42 and Rac1. Nature **367:**40–46. http://dx.doi.org/10.1038/367040a0.
3. **Arias-Romero LE, Chernoff J.** 2008. A tale of two Paks. Biol Cell **100:**97–108. http://dx.doi.org/10.1042/BC20070109.
4. **Stockton RA, Schaefer E, Schwartz MA.** 2004. p21-activated kinase regulates endothelial permeability through modulation of contractility. J Biol Chem **279:**46621–46630. http://dx.doi.org/10.1074/jbc.M408877200.
5. **Liu J, Fraser SD, Faloon PW, Rollins EL, Vom Berg J, Starovic-Subota O, Laliberte AL, Chen JN, Serluca FC, Childs SJ.** 2007. A betaPix Pak2a signaling pathway regulates cerebral vascular stability in zebrafish. Proc Natl Acad Sci U S A **104:**13990–13995. http://dx.doi.org/10.1073/pnas.0700825104.
6. **Koh W, Sachidanandam K, Stratman AN, Sacharidou A, Mayo AM, Murphy EA, Cheresh DA, Davis GE.** 2009. Formation of endothelial lumens requires a coordinated PKCepsilon-, Src-, Pak- and Raf-kinase-dependent signaling cascade downstream of Cdc42 activation. J Cell Sci **122:**1812–1822. http://dx.doi.org/10.1242/jcs.045799.
7. **Kiosses WB, Daniels RH, Otey C, Bokoch GM, Schwartz MA.** 1999. A role for p21-activated kinase in endothelial cell migration. J Cell Biol **147:**831–844. http://dx.doi.org/10.1083/jcb.147.4.831.
8. **Kelly ML, Astsaturov A, Chernoff J.** 2013. Role of p21-activated kinases in cardiovascular development and function. Cell Mol Life Sci **70:**4223–4228. http://dx.doi.org/10.1007/s00018-013-1347-8.
9. **Galan Moya EM, Le Guelte A, Gavard J.** 2009. PAKing up to the endothelium. Cell Signal **21:**1727–1737. http://dx.doi.org/10.1016/j.cellsig.2009.08.006.
10. **McDaniel AS, Allen JD, Park SJ, Jaffer ZM, Michels EG, Burgin SJ, Chen S, Bessler WK, Hofmann C, Ingram DA, Chernoff J, Clapp DW.** 2008. Pak1 regulates multiple c-Kit mediated Ras-MAPK gain-in-function phenotypes in Nf1$^{+/-}$ mast cells. Blood **112:**4646–4654. http://dx.doi.org/10.1182/blood-2008-04-155085.
11. **Meng J, Meng Y, Hanna A, Janus C, Jia Z.** 2005. Abnormal long-lasting

synaptic plasticity and cognition in mice lacking the mental retardation gene Pak3. J Neurosci **25:**6641–6650.
12. **Hofmann C, Shepelev M, Chernoff J.** 2004. The genetics of Pak. J Cell Sci **117:**4343–4354. http://dx.doi.org/10.1242/jcs.01392.
13. **Wojciak-Stothard B, Tsang LY, Paleolog E, Hall SM, Haworth SG.** 2006. Rac1 and RhoA as regulators of endothelial phenotype and barrier function in hypoxia-induced neonatal pulmonary hypertension. Am J Physiol Lung Cell Mol Physiol **290:**L1173–L1182. http://dx.doi.org/10.1152/ajplung.00309.2005.
14. **Bagheri-Yarmand R, Vadlamudi RK, Wang RA, Mendelsohn J, Kumar R.** 2000. Vascular endothelial growth factor up-regulation via p21-activated kinase-1 signaling regulates heregulin-beta1-mediated angiogenesis. J Biol Chem **275:**39451–39457. http://dx.doi.org/10.1074/jbc.M006150200.
15. **Gavard J, Gutkind JS.** 2006. VEGF controls endothelial-cell permeability by promoting the beta-arrestin-dependent endocytosis of VE-cadherin. Nat Cell Biol **8:**1223–1234. http://dx.doi.org/10.1038/ncb1486.
16. **Lampugnani MG, Zanetti A, Breviario F, Balconi G, Orsenigo F, Corada M, Spagnuolo R, Betson M, Braga V, Dejana E.** 2002. VE-cadherin regulates endothelial actin activating Rac and increasing membrane association of Tiam. Mol Biol Cell **13:**1175–1189. http://dx.doi.org/10.1091/mbc.01-07-0368.
17. **Alva JA, Zovein AC, Monvoisin A, Murphy T, Salazar A, Harvey NL, Carmeliet P, Iruela-Arispe ML.** 2006. VE-cadherin-Cre-recombinase transgenic mouse: a tool for lineage analysis and gene deletion in endothelial cells. Dev Dyn **235:**759–767. http://dx.doi.org/10.1002/dvdy.20643.
18. **Voyta JC, Via DP, Butterfield CE, Zetter BR.** 1984. Identification and isolation of endothelial cells based on their increased uptake of acetylated-low density lipoprotein. J Cell Biol **99:**2034–2040. http://dx.doi.org/10.1083/jcb.99.6.2034.
19. **Nakatsu MN, Davis J, Hughes CC.** 2007. Optimized fibrin gel bead assay for the study of angiogenesis. J Vis Exp **2007:**186. http://dx.doi.org/10.3791/186.
20. **Radu M, Chernoff J.** 2013. An in vivo assay to test blood vessel permeability. J Vis Exp **2013:**e50062. http://dx.doi.org/10.3791/50062.
21. **Stockton R, Reutershan J, Scott D, Sanders J, Ley K, Schwartz MA.** 2007. Induction of vascular permeability: beta PIX and GIT1 scaffold the activation of extracellular signal-regulated kinase by PAK. Mol Biol Cell **18:**2346–2355. http://dx.doi.org/10.1091/mbc.E06-07-0584.
22. **Garvin S, Dabrosin C.** 2003. Tamoxifen inhibits secretion of vascular endothelial growth factor in breast cancer in vivo. Cancer Res **63:**8742–8748.
23. **Risau W.** 1997. Mechanisms of angiogenesis. Nature **386:**671–674. http://dx.doi.org/10.1038/386671a0.
24. **Koh W, Mahan RD, Davis GE.** 2008. Cdc42- and Rac1-mediated endothelial lumen formation requires Pak2, Pak4 and Par3, and PKC-dependent signaling. J Cell Sci **121:**989–1001. http://dx.doi.org/10.1242/jcs.020693.
25. **Nehls V, Drenckhahn D.** 1995. A novel, microcarrier-based in vitro assay for rapid and reliable quantification of three-dimensional cell migration and angiogenesis. Microvasc Res **50:**311–322. http://dx.doi.org/10.1006/mvre.1995.1061.
26. **Yang N, Higuchi O, Ohashi K, Nagata K, Wada A, Kangawa K, Nishida E, Mizuno K.** 1998. Cofilin phosphorylation by LIM-kinase 1 and its role in Rac-mediated actin reorganization. Nature **393:**809–812. http://dx.doi.org/10.1038/31735.
27. **Nayal A, Webb DJ, Brown CM, Schaefer EM, Vicente-Manzanares M, Horwitz AR.** 2006. Paxillin phosphorylation at Ser273 localizes a GIT1-PIX-PAK complex and regulates adhesion and protrusion dynamics. J Cell Biol **173:**587–589. http://dx.doi.org/10.1083/jcb.200509075.
28. **Coniglio SJ, Zavarella S, Symons MH.** 2008. Pak1 and Pak2 mediate tumor cell invasion through distinct signaling mechanisms. Mol Cell Biol **28:**4162–4172. http://dx.doi.org/10.1128/MCB.01532-07.
29. **Antonov AS, Lukashev ME, Romanov YA, Tkachuk VA, Repin VS, Smirnov VN.** 1986. Morphological alterations in endothelial cells from human aorta and umbilical vein induced by forskolin and phorbol 12-myristate 13-acetate: a synergistic action of adenylate cyclase and protein kinase C activators. Proc Natl Acad Sci U S A **83:**9704–9708. http://dx.doi.org/10.1073/pnas.83.24.9704.
30. **Ong CC, Jubb AM, Zhou W, Haverty PM, Harris AL, Belvin M, Friedman LS, Koeppen H, Hoeflich KP.** 2011. p21-activated kinase 1: PAK'ed with potential. Oncotarget **2:**491–496. http://dx.doi.org/10.18632/oncotarget.271.
31. **Hayashi M, Kim SW, Imanaka-Yoshida K, Yoshida T, Abel ED, Eliceiri B, Yang Y, Ulevitch RJ, Lee JD.** 2004. Targeted deletion of BMK1/ERK5 in adult mice perturbs vascular integrity and leads to endothelial failure. J Clin Invest **113:**1138–1148. http://dx.doi.org/10.1172/JCI200419890.
32. **Nithianandarajah-Jones GN, Wilm B, Goldring CE, Muller J, Cross MJ.** 2012. ERK5: structure, regulation and function. Cell Signal **24:**2187–2196. http://dx.doi.org/10.1016/j.cellsig.2012.07.007.
33. **Chow HY, Dong B, Duron SG, Campbell DA, Ong CC, Hoeflich KP, Chang LS, Welling DB, Yang ZJ, Chernoff J.** 2015. Group I Paks as therapeutic targets in NF2-deficient meningioma. Oncotarget **6:**1981–1994. http://dx.doi.org/10.18632/oncotarget.2810.
34. **Kiosses WB, Hood J, Yang S, Gerritsen ME, Cheresh DA, Alderson N, Schwartz MA.** 2002. A dominant-negative p65 PAK peptide inhibits angiogenesis. Circ Res **90:**697–702. http://dx.doi.org/10.1161/01.RES.0000014227.76102.5D.
35. **Yurdagul A, Jr, Chen J, Funk SD, Albert P, Kevil CG, Orr AW.** 2013. Altered nitric oxide production mediates matrix-specific PAK2 and NF-kappaB activation by flow. Mol Biol Cell **24:**398–408. http://dx.doi.org/10.1091/mbc.E12-07-0513.
36. **Dorrance AM, De Vita S, Radu M, Reddy PN, McGuinness MK, Harris CE, Mathieu R, Lane SW, Kosoff R, Milsom MD, Chernoff J, Williams DA.** 2013. The Rac GTPase effector p21-activated kinase is essential for hematopoietic stem/progenitor cell migration and engraftment. Blood **121:**2474–2482. http://dx.doi.org/10.1182/blood-2012-10-460709.
37. **Kosoff R, Chow HY, Radu M, Chernoff J.** 2013. Pak2 kinase restrains mast cell FcepsilonRI receptor signaling through modulation of Rho protein guanine nucleotide exchange factor (GEF) activity. J Biol Chem **288:**974–983. http://dx.doi.org/10.1074/jbc.M112.422295.
38. **Arias-Romero LE, Villamar-Cruz O, Huang M, Hoeflich KP, Chernoff J.** 2013. Pak1 kinase links ErbB2 to beta-catenin in transformation of breast epithelial cells. Cancer Res **73:**3671–3682. http://dx.doi.org/10.1158/0008-5472.CAN-12-4453.
39. **Benitah SA, Frye M, Glogauer M, Watt FM.** 2005. Stem cell depletion through epidermal deletion of Rac1. Science **309:**933–935. http://dx.doi.org/10.1126/science.1113579.
40. **Van den Broeke C, Radu M, Deruelle M, Nauwynck H, Hofmann C, Jaffer ZM, Chernoff J, Favoreel HW.** 2009. Alphaherpesvirus US3-mediated reorganization of the actin cytoskeleton is mediated by group A p21-activated kinases. Proc Natl Acad Sci U S A **106:**8707–8712. http://dx.doi.org/10.1073/pnas.0900436106.
41. **Rudel T, Bokoch GM.** 1997. Membrane and morphological changes in apoptotic cells regulated by caspase-mediated activation of PAK2. Science **276:**1571–1574. http://dx.doi.org/10.1126/science.276.5318.1571.
42. **Frank SR, Bell JH, Frodin M, Hansen SH.** 2012. A betaPIX-PAK2 complex confers protection against Scrib-dependent and cadherin-mediated apoptosis. Curr Biol **22:**1747–1754. http://dx.doi.org/10.1016/j.cub.2012.07.011.
43. **Tan W, Palmby TR, Gavard J, Amornphimoltham P, Zheng Y, Gutkind JS.** 2008. An essential role for Rac1 in endothelial cell function and vascular development. FASEB J **22:**1829–1838. http://dx.doi.org/10.1096/fj.07-096438.
44. **Srinivasan R, Zabuawala T, Huang H, Zhang J, Gulati P, Fernandez S, Karlo JC, Landreth GE, Leone G, Ostrowski MC.** 2009. Erk1 and Erk2 regulate endothelial cell proliferation and migration during mouse embryonic angiogenesis. PLoS One **4:**e8283. http://dx.doi.org/10.1371/journal.pone.0008283.
45. **Wirth A, Schroeter M, Kock-Hauser C, Manser E, Chalovich JM, De Lanerolle P, Pfitzer G.** 2003. Inhibition of contraction and myosin light chain phosphorylation in guinea-pig smooth muscle by p21-activated kinase 1. J Physiol **549:**489–500. http://dx.doi.org/10.1113/jphysiol.2002.033167.
46. **Reutershan J, Stockton R, Zarbock A, Sullivan GW, Chang D, Scott D, Schwartz MA, Ley K.** 2007. Blocking p21-activated kinase reduces lipopolysaccharide-induced acute lung injury by preventing polymorphonuclear leukocyte infiltration. Am J Respir Crit Care Med **175:**1027–1035. http://dx.doi.org/10.1164/rccm.200612-1822OC.
47. **Birukova AA, Zagranichnaya T, Alekseeva E, Bokoch GM, Birukov KG.** 2008. Epac/Rap and PKA are novel mechanisms of ANP-induced Rac-mediated pulmonary endothelial barrier protection. J Cell Physiol **215:**715–724. http://dx.doi.org/10.1002/jcp.21354.
48. **Buchner DA, Su F, Yamaoka JS, Kamei M, Shavit JA, Barthel LK, McGee B, Amigo JD, Kim S, Hanosh AW, Jagadeeswaran P, Goldman D, Lawson ND, Raymond PA, Weinstein BM, Ginsburg D, Lyons SE.**

2007. pak2a mutations cause cerebral hemorrhage in redhead zebrafish. Proc Natl Acad Sci U S A **104:**13996–14001. http://dx.doi.org/10.1073/pnas.0700947104.

49. **Pi X, Garin G, Xie L, Zheng Q, Wei H, Abe J, Yan C, Berk BC.** 2005. BMK1/ERK5 is a novel regulator of angiogenesis by destabilizing hypoxia inducible factor 1alpha. Circ Res **96:**1145–1151. http://dx.doi.org/10.1161/01.RES.0000168802.43528.e1.
50. **Sohn SJ, Sarvis BK, Cado D, Winoto A.** 2002. ERK5 MAPK regulates embryonic angiogenesis and acts as a hypoxia-sensitive repressor of vascular endothelial growth factor expression. J Biol Chem **277:**43344–43351. http://dx.doi.org/10.1074/jbc.M207573200.
51. **Pi X, Yan C, Berk BC.** 2004. Big mitogen-activated protein kinase (BMK1)/ERK5 protects endothelial cells from apoptosis. Circ Res **94:**362–369. http://dx.doi.org/10.1161/01.RES.0000112406.27800.6F.
52. **Rovida E, Navari N, Caligiuri A, Dello Sbarba P, Marra F.** 2008. ERK5 differentially regulates PDGF-induced proliferation and migration of hepatic stellate cells. J Hepatol **48:**107–115. http://dx.doi.org/10.1016/j.jhep.2007.08.010.
53. **Komaravolu RK, Adam C, Moonen JR, Harmsen MC, Goebeler M, Schmidt M.** 2015. Erk5 inhibits endothelial migration via KLF2-dependent downregulation of PAK1. Cardiovasc Res **105:**86–95. http://dx.doi.org/10.1093/cvr/cvu236.